ORIGINAL ARTICLE

Augmented reality headsets for surgical guidance: the impact of holographic model positions on user localisation accuracy

Laura Pérez-Pachón[1] · Parivrudh Sharma[2] · Helena Brech[1] · Jenny Gregory[1] · Terry Lowe[3] · Matthieu Poyade[4] · Flora Gröning[1]

Abstract
Novel augmented reality headsets such as HoloLens can be used to overlay patient-specific virtual models of resection margins on the patient's skin, providing surgeons with information not normally available in the operating room. For this to be useful, surgeons wearing the headset must be able to localise virtual models accurately. We measured the error with which users localise virtual models at different positions and distances from their eyes. Healthy volunteers aged 20–59 years ($n = 54$) performed 81 exercises involving the localisation of a virtual hexagon's vertices overlaid on a monitor surface. Nine predefined positions and three distances between the virtual hexagon and the users' eyes (65, 85 and 105 cm) were set. We found that, some model positions and the shortest distance (65 cm) led to larger localisation errors than other positions and larger distances (85 and 105 cm). Positional errors of more than 5 mm and 1–5 mm margin errors were found in 29.8% and over 40% of cases, respectively. Strong outliers were also found (e.g. margin shrinkage of up to 17.4 mm in 4.3% of cases). The measured errors may result in poor outcomes of surgeries: e.g. incomplete tumour excision or inaccurate flap design, which can potentially lead to tumour recurrence and flap failure, respectively. Reducing localisation errors associated with arm reach distances between the virtual models and users' eyes is necessary for augmented reality headsets to be suitable for surgical purposes. In addition, training surgeons on the use of these headsets may help to minimise localisation errors.

Keywords Image marker · Augmented reality · Surgery · Surgical navigation · Augmented reality headsets · Skin tumour removal

1 Introduction

Novel augmented reality (AR) headsets are wearable devices with see-through displays that can render virtual models aligned with real world features (Kress and Cummings 2017b; Park et al. 2021). Alignment may be achieved by using physical image markers that are captured by the headset's camera, which triggers the rendering of virtual models on the headset's lenses in a predefined position (Benmahdjoub et al. 2022). This technology can be used to guide surgeons, during the resection of soft tissues by overlaying patient-specific virtual models obtained from medical scans on the patient (Park et al. 2021; Castelan et al. 2021). This application is especially interesting for oncological surgery, where complete tumour removal is key to preventing tumour recurrence. In addition, this technology may enhance the design of free flaps during reconstructive surgery; free flaps are vascularised tissue that is transferred from one part of a patient's body to the site of a defect to reconstruct anatomical structures that have been damaged, e.g. after tumour removal (Pratt et al. 2018). For this application to be useful, surgeons wearing the headset must be able to localise virtual models accurately. The present study measured the user localisation error (i.e. the difference between the perceived position of features on the virtual models and their actual position), as well as errors in the perceived position and size of the virtual models as a whole and discusses the

✉ Parivrudh Sharma
  parivrudh.sharma1@nhs.net

[1] School of Medicine, Medical Sciences and Nutrition, University of Aberdeen, Aberdeen, UK

[2] Princess Royal Hospital, Brighton and Sussex University Hospitals NHS Trust, Haywards Heath, UK

[3] Head and Neck Oncology Unit, Aberdeen Royal Infirmary (NHS Grampian), Aberdeen, UK

[4] School of Simulation and Visualisation, Glasgow School of Art, Glasgow, UK

potential effect of these errors on the outcomes of surgeries that involve the resection of superficial soft tissues.

1.1 The challenge of accurate soft tissue resection in oncological and reconstructive surgery

Accurate soft tissue resection is critical for surgical success as optimal resection margins are considered the most important factor for tumour control and prevention of repeat intervention (Sheoran et al. 2022; Sugiura et al. 2018).

Soft tissue free flaps are vascularized soft tissue (i.e. skin, fascia and sometimes muscle) transferred from one part of a patient's body to the site of a defect to restore the function of damaged anatomical structures (Hallock 2009). Perforator vessels originate in a main source artery, pierce the deep fascia (a layer of dense connective tissue that surrounds muscles) and branch into subcutaneous vessels (Higueras Suñé et al. 2011). The accurate localisation of perforator vessels is key to preventing impaired blood flow and flap necrosis (Wilson et al. 2009). Flaps must also have adequate shape and dimensions to fit defects. Oversized flaps may create noticeably raised flap tissue compared to the surrounding tissue after their attachment to the site of the defect (Klaassen et al. 2018). Undersized flaps are prone to distortions due to tissue tension and contraction during the healing process, thus increasing the risk of flap necrosis and/or undesired aesthetic results (Feng et al. 2017). To prevent undersized flaps, surgeons normally add a portion of tissue surrounding the flap, e.g. 5 mm (Feng et al. 2017). If the resulting flap is oversized, surgeons trim the flap before its attachment to the site of the defect. A real time image guidance tool for flap design does not exist yet, thus surgeons mainly rely on the visual inspection of the patients' anatomy to accomplish these tasks, which may lead to extended flap raising and surgery times (Ishii and Kishi 2016).

The excision of small tumours requires submillimetre accuracy (Ghosh et al. 2014). Before the resection of skin and subcutaneous tumour tissue, surgeons delineate tumour margins using tools such as marker pens, rulers and loupes with percentage errors of 8–45% relative to the planned margins (Lalla et al. 2003). Delineation errors as well as the incorrect mapping of tumours may lead to their incomplete excision, which is associated with high recurrence rates, e.g. up to 55% and 60% in basal cell carcinoma and breast tumours, respectively (Waljee et al. 2008; Ríos-Buceta 2007). Incomplete excision may also lead to repeat surgery and increased morbidity, e.g. if critical anatomical structures are damaged (Telfer et al. 2008), and thus additional hospital expenses and a higher risk of complications for patients (Richmond and Davie 1987).

AR-guided localisation of perforator vessels has been investigated in previous studies (Bosc et al. 2017; Jiang et al. 2017; Pratt et al. 2018). However, to the authors' knowledge, only one study explored the use of AR to indicate planned resection margins of flaps via conventional projection (Hummelink et al. 2017). Previous studies have also explored the AR-guided assessment of tumour resection margins. For instance, Shao et al. (2014) developed a system that used wearable technology to assist surgeons in the identification of tumour margins. This system had the sensitivity and specificity of commercial fluorescence imaging systems. Similarly, Cui et al. (2017) presented a system that rendered fluorescent images on the lenses of an AR headset. They highlighted the potential of this technology to provide an AR visualisation of tumours without blocking the surgeon's view.

1.2 Limitations of current research

Most previous studies on AR-guided surgery did not study the effect of two variables on the user localisation error: (1) the user's viewing angle of the virtual models, and (2) the distance between the virtual models and the user's eyes (Frantz et al. 2018). These variables change with the surgeon's movement around the patient and thus their effect must be investigated. Luzon et al. (2020) explored the impact of the surgeon's viewing angle while wearing an AR device, but conclusions should be drawn with caution considering the small sample size of five participants and that the participants' head position and distance from the markers were not controlled, so that these variables might have influenced the results. Previous studies have often performed accuracy tests under simulated surgical scenarios. Simulations of clinical scenarios are necessary to evaluate AR surgical guidance systems (Pérez-Pachón et al. 2020), but limit the number and type of measurements and number of participants that can be included in the analyses due to the complexity of the experimental design (Herzog et al. 2019). In addition, measuring localisation errors during a surgical task includes variations in the participants' expertise and dexterity as additional sources of error (Bann et al. 2003; Sondak and Zager 2010). Moreover, X-ray vision (i.e. the perception that virtual models of internal anatomical structures lie on the surface of the patient) is a common problem in AR applications for surgery and may lead to localisation errors (Avery et al. 2009).

1.3 Aims

This study measured the error with which users of an AR headset localise virtual models aligned with real world features. A simple setup was used to reduce perception issues typically associated with X-ray vision and to facilitate a large sample size and thus the collection of a

sufficiently large number of measurements for statistical testing. The research questions were:

(RQ1) What is the error in the users' localisation of virtual models and to what extent does it result in errors in the perceived position and dimensions of the virtual models?

(RQ2) Is there a relationship between these errors and the position and distance of the virtual models from the user's eyes?

2 Methods

2.1 Participants

We recruited 54 adults aged 20–59 years from staff and students at the University of Aberdeen for this study. All those selected were in good health and without vision problems except those corrected by glasses or contact lenses. The sample size was determined following the results of a power analysis for an ANOVA using *G**Power (Faul et al. 2007).

2.2 Experimental setup

The first generation of the AR headset HoloLens (Microsoft Corporation, Redmond, USA) was used in the experiment as the equipment was purchased at the beginning of our project prior to the release of HoloLens 2. An AR app (App-1) was created using Vuforia Engine (Kress and Cummings 2017a). App-1 allowed for the detection of a 12×12 cm digital image marker (referred to as "marker" henceforth) by the headset's camera. This triggered the rendering of a virtual model (a 5-cm-radius virtual hexagon) on the headset's lenses in a set position (Fig. 1a). The virtual hexagon was rendered as an opaque figure because transparency has been reported to create issues in the users' perception of the virtual models' position (Kersten-Oertel et al. 2012). A second app (App-2) was run on a laptop connected to the monitor. App-2 displayed the marker on a monitor in random order at one out of nine predefined positions (Fig. 1a). For the assessment of the observation distance (i.e. the distance between the virtual models and the user's eyes) on the localisation error, three different distances (distances 1–3) between the monitor and the headset's camera were set: 65, 85 and 105 cm, respectively (Fig. 1b). Red marks on a table that matched distances 1–3 were used to ensure

Fig. 1 Diagrams of **a** the frontal view of the experimental setup showing a monitor displaying 12×12 cm digital image markers at positions 1–9 and virtual hexagons rendered on the headset's lenses at the positions where we predicted that users would perceive them (i.e. overlaid on the monitor surface and aligned with their corresponding digital image marker); and **b** the top view showing the monitor at distances 1–3 (i.e. 65, 85 and 105 cm, respectively) and the virtual hexagons (red arrows) and; **c** photo showing the experimental setup and a researcher adjusting the position of the monitor. Image marker positions 1–8 were at 108 mm from the centre of the monitor and position 9 was aligned with the centre of the monitor
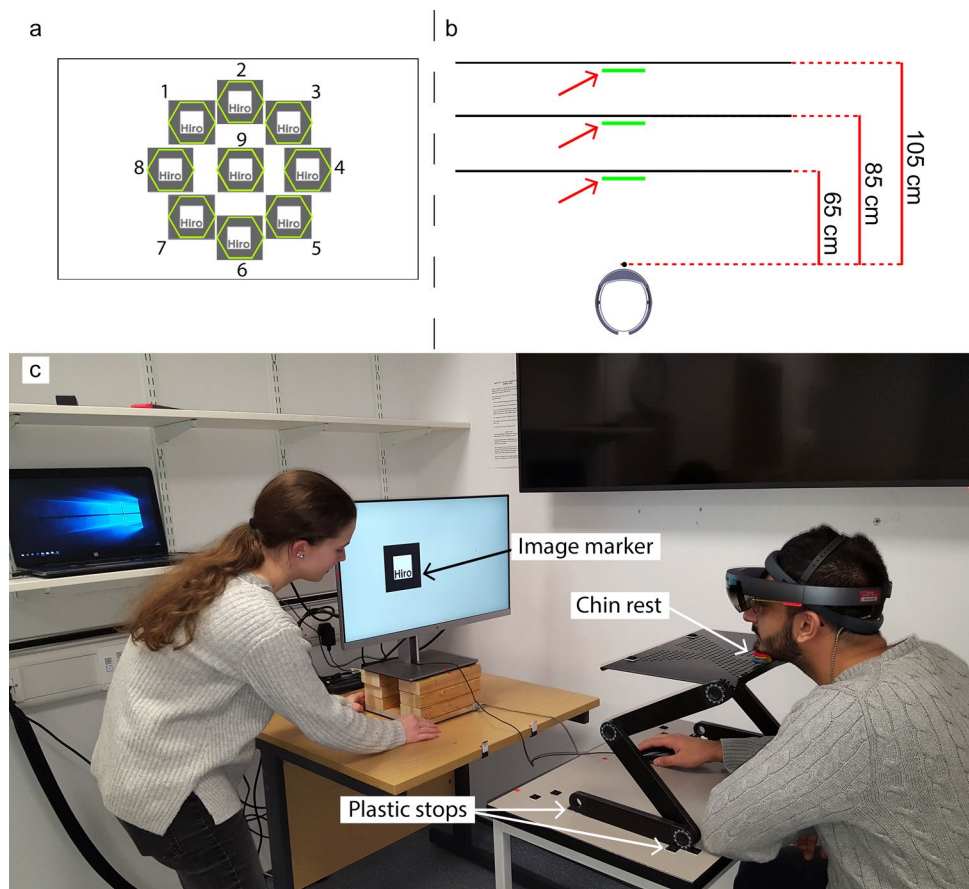
the correct position of the monitor (Online Resource 1). To measure the intraobserver error, each participant performed the exercises three times. With the combination of marker positions, monitor-camera distances and repeated measures, each participant completed 81 exercises. A chin rest on a lectern was used to ensure that the head of each participant was in the correct position and remained in this position (Fig. 1c). Plastic stops ensured the correct position of the lectern. The chin rest was aligned with the vertical midline of the monitor surface.

2.3 Procedure

The experiment was conducted under controlled lighting conditions. Participants were asked to adjust the headset to the distance between their eyes (using the HoloLens calibration app) and place their chin on the chin rest (Fig. 1). The centre of the monitor was aligned with the headset camera by placing the monitor at distance one and displaying a digital graph chart, and then placing a laser measuring tool (including a level indicator to ensure its horizontal position) in front of the headset camera pointing at the digital graph chart. A researcher held the laser measuring tool, while another researcher adjusted the monitor height to match the centre of the digital graph chart with the laser pointer. The monitor was levelled to ensure that its screen surface was perpendicular to the headset's camera plane. This process ensured that the predicted positions and distances of the virtual hexagons from the participants' eyes remained constant during the experiment (Fig. 2). After these adjustments, the digital graph chart was removed.

For each exercise, the monitor was placed at the corresponding distance from the headset camera. Once the headset camera detected a marker, a virtual hexagon was rendered on the headset lenses. If the system performance and participants' perception were error-free, the virtual hexagon would

be perceived by participants at its predefined position (Fig. 1a). Then, the marker was removed from the visualisation and participants were asked to click on each vertex of the virtual hexagon using a mouse. The x- and y-coordinates of each click were recorded by App-2.

2.4 Data analysis

Vertex localisation errors were expected to generate errors in the virtual hexagons' position and dimensions (Online Resource 2). SPSS 25 (IBM Statistics, Chicago, USA) and SigmaPlot 14 (Systat Software, San Jose, CA) were used for statistical analysis. The participants' clicks were used to calculate the error in the position of the virtual hexagons' vertices:

$$Verr_n = \sqrt{\left[(x - x')^2 + (y - y')^2\right]} \tag{1}$$

$$\mu_{Verr} = \frac{(eV^{n1} + eV^{n2} + eV^{n3} + eV^{n4} + eV^{n5} + eV^{n6})}{6}, \tag{2}$$

where $Verr_n$ is the error in the position of a given virtual hexagon's vertex, x and y are the predicted x and y coordinates, respectively, x' and y' are the x and y coordinates of the participants' clicks, respectively, and μ_{Verr} is the mean error in the position of the virtual hexagon's vertices.

The participant's clicks were also used to calculate the error in the virtual hexagons' area. As the virtual hexagons as perceived by the participants were expected to be irregular polygons, the area was obtained by calculating the sum of the areas of the four triangles forming the virtual hexagons (Online Resource 3), for which the following formulae were used:

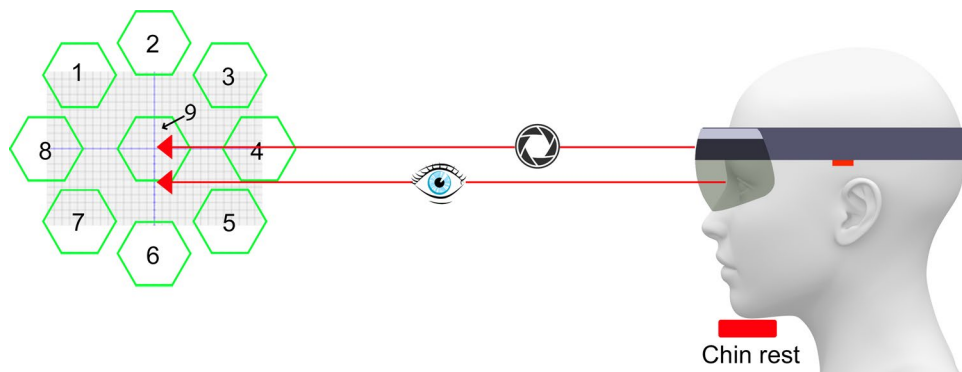$$s = \frac{(a + b + c)}{2} \tag{3}$$

Fig. 2 Experimental setup showing a participant wearing the HoloLens headset with their chin on the chin rest, the headset's camera aligned with the centre of the digital graph chart and their eyes aligned with the digital graph chart and virtual hexagons. In this experimental setup, the participant observes the hexagon from their perspective; however, the participant only sees one rendered hexagon at a time on the grid

$$A_n = \sqrt{s(s-a)(s-b)(s-c)} \tag{4}$$

$$hA = A_1 + A_2 + A_3 + A_4, \tag{5}$$

where s is the semi-perimeter of a given triangle, a, b and c are the length of its sides, A is the triangle's area, and hA is the virtual hexagon's area.

In addition, the participant's clicks were used to calculate the error in the virtual hexagons' centroid position:

$$C_x' = \frac{1}{6hA} \sum_{i=0}^{n-1} [(x_i + x_{i+1})(x_i y_{i+1} - x_{i+1} y_i)] \tag{6}$$

$$C_y' = \frac{1}{6hA} \sum_{i=0}^{n-1} [(y_i + y_{i+1})(x_i y_{i+1} - x_{i+1} y_i)] \tag{7}$$

$$C\mathrm{err} = \sqrt{(C_x - C_x')^2 + (C_y - C_y')^2}, \tag{8}$$

where C_x' and C_y' are the x and y coordinates, respectively, of the centroid defined by the vertex positions of the hexagon marked by the participant, hA is the virtual hexagon's area, $C\mathrm{err}$ is the error in the centroid position, and C_x and C_y are the predefined x and y coordinate of the centroid, respectively.

The virtual hexagons' area was also used to calculate the expansion or shrinkage of the perceived hexagon (i.e. the "margin error") by calculating the long diagonal and comparing it with its predicted length:

$$D = 2\sqrt{\frac{pA}{1.5\sqrt{3}}} \tag{9}$$

$$D' = 2\sqrt{\frac{hA}{1.5\sqrt{3}}} \tag{10}$$

$$M = \frac{D - D'}{2}, \tag{11}$$

where D' is the predicted length of the long diagonal, pA is the predicted area, D' is the length of the long diagonal of the virtual hexagon, hA is the virtual hexagon's area and M is the margin error. This calculation assumed that the virtual hexagons remained regular polygons after changes in their area and thus changes in the virtual hexagons' shape were not considered. A summary of the independent and dependent variables is provided in online resource 4. The intraclass correlation coefficient (ICC) was used to analyse the intraobserver variability in the vertex localisation error (Koo and Li 2016). Since, data were not normally distributed, a

non-parametric Kruskal–Wallis H test ($p < 0.001$) was used to analyse the differences between participants.

Errors exceeding 1.5- and 3-times the interquartile range (IQR) were classified as weak and strong outliers (Hoaglin et al. 1986), respectively. Errors across groups were compared within each independent variable (i.e. the predicted positions and distances of the virtual hexagons from the participant's eyes). For comparisons between more than two groups, the non-parametric Kruskal–Wallis H test ($p < 0.001$) was used and subsequent pairwise comparisons were performed using Dunn's method ($p < 0.05$). Three error categories ($\leq 0.5, \leq 1$ and ≤ 5 mm) were determined for the centroid position and margin errors, respectively; these margin errors corresponded to area errors of $\leq 2.0, \leq 4.1$ and $\leq 21.0\%$, respectively. The percentage of errors within each category was then calculated. These categories allowed exploring the frequency of: submillimetre errors required for high-precision surgery such as tumour excision, ophthalmology, otology, or micro-reconstructive surgery (Mattos et al. 2016); and ≤ 5 mm errors, which may be acceptable for some surgical tasks such as the preoperative staging of breast cancer tumours (Luparia et al. 2013).

3 Results

3.1 Error in the users' localisation of virtual models

Results obtained for each participant revealed a high similarity between repetitions (ICC = 0.9). In contrast, the vertex localisation error was significantly different between participants ($p < 0.001$), showing a wide error range and 1.8% of outliers (Online Resource 5). This suggests that vertex localisation errors were user-dependent. Based on the assumption that strong outliers are likely to be easily detected as incorrect by surgeons (Online Resource 6), we excluded strong outliers from subsequent analyses. Overall, average vertex localisation, centroid position and margin errors all remained below 5 mm (Table 1). Additionally, the absolute and relative average errors of percentage area were found to be 3.8% and 1.6%, respectively. 1–5 mm and over 5 mm centroid position errors were found in 64.4% and 29.8% of cases, respectively, when observed from a 65 cm distance (Table 2). Errors in the virtual hexagons' margins remained below 5 mm, with 72.2% and 27.8% of the hexagons' margins showing an expansion or shrinkage, respectively.

3.2 Effect of the virtual models' position relative to the users' eyes

The effect of virtual hexagon position on vertex localisation, centroid position and absolute area errors is summarised in Fig. 3a. Vertex localisation and centroid position errors were

Table 1 Errors for all dependent variables including all virtual hexagon positions and distances from the participants' eyes.

		Min	Max	Mean	SD
Vertex localisation (mm)		0.7	14.8	4.3	2.3
Centroid position (mm)		0.1	14.9	4.1	2.5
Area (%)	Absolute	0	15	3.8	2.7
	Relative	− 14.7	15	1.6	4.3
Margins (mm)	Absolute	0	3.8	0.9	0.7
	Relative	− 3.8	3.6	0.4	1.1

Strong outliers (i.e. values > 3 IQR) were excluded. Absolute values show the extent of the change in the hexagon size, while relative values reflect a trend for the hexagon to shrink or expand across multiple localisation attempts from the participants

Table 2 Percentage of virtual hexagons showing ≤ 0.5, ≤ 1 and ≤ 5 mm centroid position and margins error for virtual hexagons at distance 1 (65 cm) and virtual hexagon positions 1–9 ($n = 4146$)

		Error	Percentage
Centroid position (mm)		≤ 0.5	1.4
		≤ 1	5.8
		≤ 5	70.2
Margins (mm)	Increase ($n = 2994$)	≤ 0.5	26.1
		≤ 1	60.5
		≤ 5	100
	Reduction ($n = 1152$)	≤ 0.5	41.1
		≤ 1	61.1
		≤ 5	100

Strong outliers (i.e. values > 3 IQR) were excluded

significantly different between all virtual hexagon positions ($p < 0.001$). Most participants localised the virtual hexagons on the right side of their field of vision more accurately than on the left side. Indeed, virtual hexagon positions 3, 4 and 5 (i.e. on the right side of the participant's field of view) and 6 (i.e. on the bottom side of the participant's field of view) produced significantly smaller vertex localisation and centroid position errors ($p < 0.05$) than the other virtual hexagon positions (Fig. 3b and Online Resource 7). In contrast, area errors were significantly smaller ($p < 0.05$) for virtual hexagon positions 1, 2, 3, 8 and 9, i.e. generally, on the viewers' eye level and above this level (Fig. 3c).

3.3 Effect of the distance between the virtual models and the users' eyes

Errors in vertex localisation and centroid position decreased as the distance between the headset's camera and the monitor increased (Fig. 4a and Online Resource 8). These errors were significantly different ($p < 0.001$) between distances 1–3 (i.e. 65, 85, and 105 cm, respectively). Distances 2

and 3 produced smaller absolute area errors than distance 1 (Fig. 4b).

4 Discussion

This study measured the errors in the perceived position and dimensions of virtual models by users of the HoloLens 1 headset and investigated the relationship between these errors and the virtual models' position and distance from the users' eyes. An increased localisation accuracy for virtual hexagons on the right side of the field of view was found (Fig. 3). This may be partially due to ocular dominance, i.e. the tendency of individuals to favour visual input from one eye, typically the eye with which visual information is perceived more clearly (Lopes-Ferreira et al. 2013). Ocular dominance occurs in 97% of individuals of which 65% show a dominant right eye (Reiss 1997).

Vertex localisation and area errors were larger for the shortest distance of the virtual hexagons from the participants' eyes (65 cm) than for larger distances, i.e. 85 and 105 cm (Fig. 4). A reason for this may be that a 65 cm distance lies outside the optimal zone for the visualisation of virtual content with HoloLens 1, which was determined as 125–200 cm from the eyes by Condino et al. (2018), and lies further from this zone than 85 and 105 cm distances. Another reason may be a reduced viewing quality of the virtual models if users observe them from short distances (Bach et al. 2018).

Centroid position errors over 5 mm represent a risk of incorrect localisation of perforator vessels during soft tissue flap surgery, which may lead to accidental injury to these vessels, thus compromising flap viability (Corbitt et al. 2014). In addition, the observed margins error, with strong outliers in 4.3% of cases (Online Resource 6), are larger than in surgeons' drawings of skin tumour resection margins using traditional tools (surgical markers, rulers and loupes), which have been reported to be around 1 mm (Lalla et al. 2003). The observed centroid position errors and margin shrinkage combined may compromise the complete excision of skin tumours or cause the inaccurate mapping of subcutaneous tumours (Table 2). The European Organization for Research and Treatment of Cancer (EORTC) reports a 17.5% cumulative incidence of tumour recurrence associated with incomplete tumour excision (Poortmans et al. 2009). Therefore, the risk for potential errors over 1 mm must be carefully considered before implementing the use of AR headsets in clinical practice.

It should be noted as a study limitation that a 12×12 cm marker was used as opposed to previous studies that used smaller markers (Luzon et al. 2020). Small markers are preferable for surgery, because they have a lower risk of occluding the surgical working area and thus interfering with

Fig. 3 Virtual hexagon positions with smallest errors for vertex localisation, centroid position and absolute area (highlighted in green) and their mean errors (**a**) and vertex localisation (**b**) and absolute area (**c**) errors for virtual hexagon positions 1–9 ($n = 4146$). Whiskers indicate ± 1.5 IQR. Weak outliers (i.e. values > 1.5 IQR and < 3 IQR) are indicated with circles and virtual hexagon positions with significantly smaller errors ($p < 0.05$) with asterisks (Kruskal Wallis H test). Strong outliers (i.e. values > 3 IQR) were excluded

Mean vertex localisation error: 4 ±2.1 mm
Mean centroid position error: 3.7 ±2.3 mm

Mean absolute area error: 3.5 ±2.6 mm
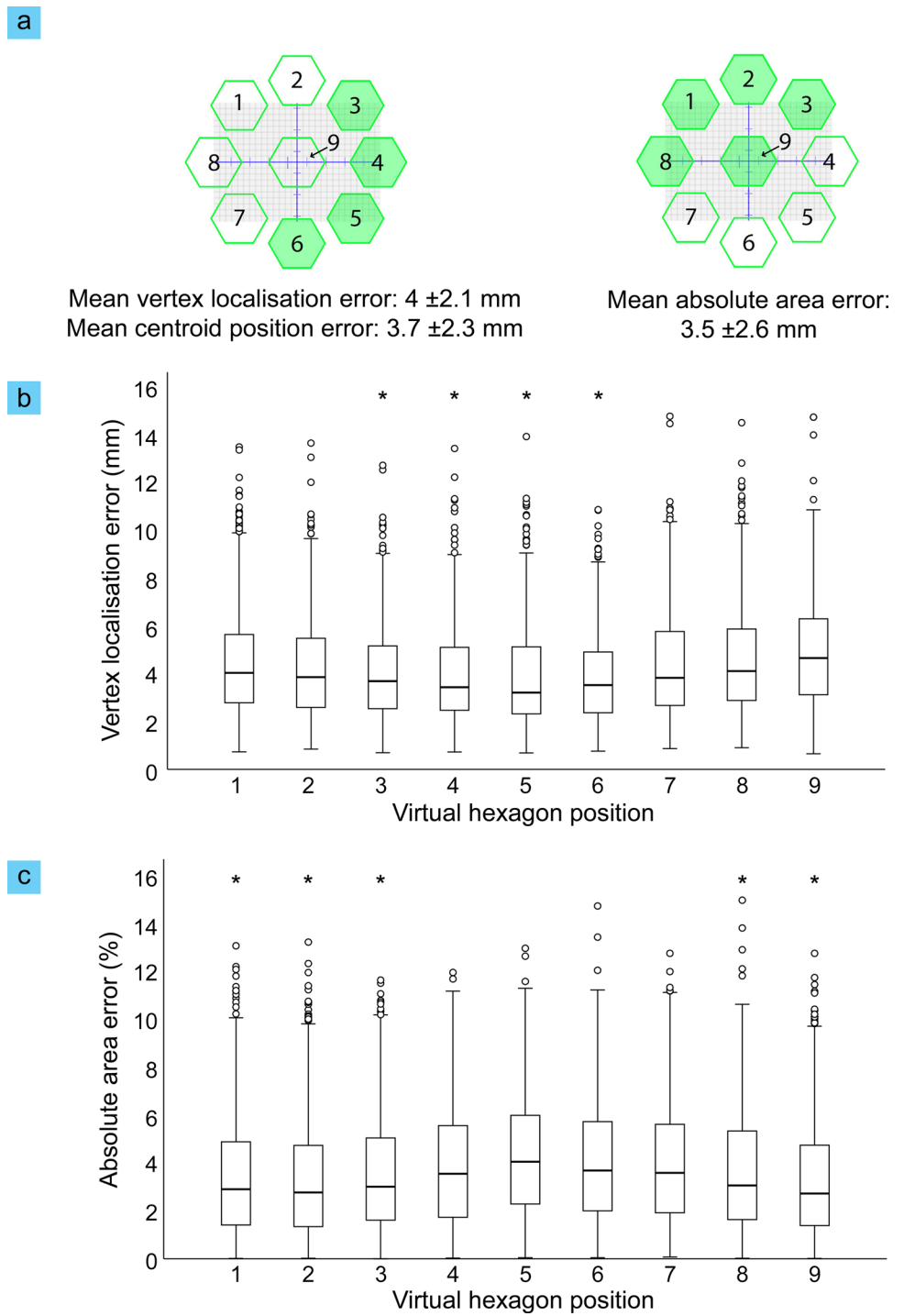
surgical workflows. However, small markers may also lead to errors that are not acceptable for surgery (Pérez-Pachón et al. 2021). In addition, our study did not include surgeon participants. Surgeons usually have increased dexterity compared to non-surgeons, due to their surgical training, and thus they are expected to show smaller errors (Sadideen et al. 2013). Moreover, this study did not measure changes in the hexagon shape, although this information would help

to prevent complications derived from mismatches between flaps and defects (Kimura 2009). Finally, our results are limited to HoloLens 1 and cannot be generalised to other headsets.

Experiments analysing user accuracy with AR headsets inform the research community and healthcare professionals on the readiness of AR technologies for their use in the operating theatre. Additional key aspects to be considered include
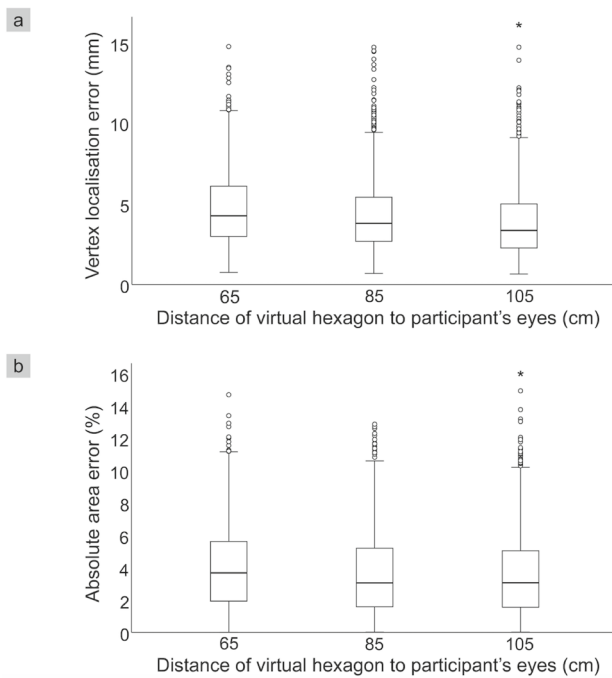
Fig. 4 Vertex localisation (**a**) and absolute area (**b**) errors for distances 1–3 ($n = 4146$). Whiskers indicate ± 1.5 IQR. Weak outliers (i.e. values > 1.5 IQR and < 3 IQR) are indicated with circles and distance associated with the smallest errors ($p < 0.05$) with asterisks (Kruskal Wallis H test). Strong outliers (i.e. values > 3 IQR) were excluded

usability, reliability, and workflow. These aspects, with accuracy likely being the next key barrier for implementation in the surgical arena, are especially relevant within the context of high-precision surgical tasks. Extensive research has explored this topic for a wide variety of surgical fields such as neurosurgery, cranio-maxillofacial surgery, or cardiovascular medicine (Gsaxner et al. 2023). With the advent of AR technologies tailored to surgical practice, HoloLens-like technology are expected to become an integral part of high-precision surgical setups within the next decade (Zhang et al. 2023).

Due to the abstract nature of our experiment, our results can also be applied to other fields that involve high-precision tasks. Research on the application of HoloLens-like technologies to high-precision tasks outside of healthcare is currently limited, however, the authors expect that there will be applications within the fields of engineering, manufacturing, and repair in the near future.

5 Conclusion

In this study, we found that some model positions and the shortest distance (65 cm) led to larger localisation errors than other positions and larger distances. Localisation errors tended to be smaller for virtual models rendered on the right side of the user's field of view. Adjusting the location of virtual models according to this may help to maximise localisation accuracy. Developers and manufacturers should also aim for minimising localisation errors for distances of 65 cm or less between the user's eyes and the virtual models, especially considering open surgery applications, where surgeons operate at an arm range distance from the surgical working area. Finally, the user-dependent errors found in this study indicate that training surgeons on the use of AR headsets may potentially help to minimise localisation errors.

Authors' contributions Study conception was done by LP, FG, MP; Experiment planning and design were done by LP, FG, MP, JG; Development of App-1 were done by LP; Development of App-2 were done by LP, MP; Data collection and analysis and first draft of the manuscript were done by LP, HB, PS; Editing: all authors.

Data availability Data supporting the findings of this study are available from the corresponding author (LP) upon reasonable request.

Code availability For the code, please contact the corresponding author.

Declarations

Conflict of interest The authors declare that they have no conflict of interest. They have no affiliations with or involvement in any organization or entity with any financial interest or non-financial interest in the subject matter or materials discussed in this manuscript.

Ethics approval The experiment was approved by the College of Life Sciences and Medicine Ethics Review Board (CERB) of the University of Aberdeen (CERB/2019/9/1824).

Consent to participate Participants of this study were given detailed information about the experiment. They then completed and signed a consent form before their participation.

References

Avery B, Sandor C, Thomas BH (2009) Improving spatial perception for augmented reality X-ray vision. IEEE Virtual Real Conf 2009:79–82

Bach B, Sicat R, Beyer J, Cordeil M, Pfister H (2018) The hologram in my hand: How effective is interactive exploration of 3D visualizations in immersive tangible augmented reality? IEEE Trans Vis Comput Graph 24:457–467

Bann SD, Khan MS, Darzi AW (2003) Measurement of surgical dexterity using motion analysis of simple bench tasks. World J Surg 27:390–394

Benmahdjoub M, Niessen WJ, Wolvius EB, van Walsum T (2022) Multimodal markers for technology-independent integration of augmented reality devices and surgical navigation systems. Virtual Real 26:1637–1650

Bosc R, Fitoussi A, Pigneur F, Tacher V, Hersant B, Meningaud JP (2017) Identification of perforating vessels by augmented reality: Application for the deep inferior epigastric perforator flap. Ann Chir Plast Esthet 62:336–339

Castelan E, Margarita V, Xianlian AZ (2021) Augmented reality anatomy visualization for surgery assistance with HoloLens: AR surgery assistance with HoloLens. In ACM international conference on interactive media experiences, pp 329–331. Virtual Event, USA: Association for Computing Machinery

Condino S, Turini G, Parchi PD, Viglialoro RM, Piolanti N, Gesi M, Ferrari M, Ferrari V (2018) How to build a patient-specific hybrid simulator for orthopaedic open surgery: benefits and limits of mixed-reality using the Microsoft HoloLens. J Healthc Eng 2018:5435097

Corbitt C, Skoracki RJ, Yu P, Hanasono MM (2014) Free flap failure in head and neck reconstruction. Head Neck 36:1440–1445

Cui N, Pradosh K, Viktor G (2017) Augmented reality with Microsoft HoloLens holograms for near infrared fluorescence based image guided surgery. In: Proceedings of SPIE 10049, molecular-guided surgery: molecules, devices, and applications III

Faul F, Erdfelder E, Lang A-G, Buchner A (2007) G*Power 3: a flexible statistical power analysis program for the social, behavioral, and biomedical sciences. Behav Res Methods 39:175–191

Feng S, Zhang Z, Xi W, Lazzeri D, Fang Y, Zhang Yi (2017) Pre-expanded bipedicled supratrochlear perforator flap for simultaneous reconstruction of the nasal and upper lip defects. Clin Plast Surg 44:153–162

Frantz T, Jansen B, Duerinck J, Vandemeulebroucke J (2018) Augmenting Microsoft's HoloLens with vuforia tracking for neuronavigation. Healthc Technol Lett 5:221–225

Ghosh D, Bagley AF, Na YJ, Birrer MJ, Bhatia SN, Belcher AM (2014) Deep, noninvasive imaging and surgical guidance of submillimeter tumors using targeted M13-stabilized single-walled carbon nanotubes. Proc Natl Acad Sci USA 111:13948–13953

Gsaxner C, Li J, Pepe A, Jin Y, Kleesiek J, Schmalstieg D, Egger J (2023) The HoloLens in medicine: a systematic review and taxonomy. Med Image Anal 85:102757

Hallock GG (2009) CHAPTER 2—Classification of flaps. In: Fu-Chan W, Samir M (eds) Flaps and reconstructive surgery. W.B. Saunders, Edinburgh

Herzog MH, Gregory F, Aaron C (2019) Experimental design: model fits, power, and complex designs. In: Herzog MH, Francis G,

Clarke A (eds) Understanding statistics and experimental design : How to not lie with statistics? Springer International Publishing, Cham

Higueras Suñé MC, López Ojeda A, Narváez García JA, De Albert De M, Las Vigo O, Roca Mas D, Perez Sidelnikova C, Carrasco López JA, Palacin Porte JM, Payró S, Viñals JM (2011) Use of angioscanning in the surgical planning of perforator flaps in the lower extremities. J Plast Reconstr Aesthet Surg 64:1207–1213

Hoaglin DC, Iglewicz B, Tukey JW (1986) Performance of some resistant rules for outlier labeling. J Am Stat Assoc 81:991–999

Hummelink S, Verhulst AC, Maal TJJ, Hoogeveen YL, Schultze Kool LJ, Ulrich DJO (2017) An innovative method of planning and displaying flap volume in DIEP flap breast reconstructions. J Plast Reconstr Aesthet Surg 70:871–875

Ishii N, Kishi K (2016) Determining length and position of pedicle vessels using a flap model with vascular tape. Plast Reconstr Surg Glob Open 4:e1161–e1261

Jiang T, Zhu M, Zan T, Gu B, Li Q (2017) A novel augmented reality-based navigation system in perforator flap transplantation—a feasibility study. Ann Plast Surg 79:192–196

Kersten-Oertel M, Chen SS, Drouin S, Sinclair DS, Collins DL (2012) Augmented reality visualization for guidance in neurovascular surgery. Stud Health Technol Inform 173:225–229

Kimura N (2009) CHAPTER 10—thinning and tailoring. In: Wei F-C, Mardini S (eds) Flaps and reconstructive surgery. W.B. Saunders, Edinburgh

Klaassen MF, Earle B, Felix B (2018) Rotation flaps. In: Klaassen MF, Brown E, Behan F (eds) Simply local flaps. Springer International Publishing, Cham

Koo TK, Mae YL (2016) A guideline of selecting and reporting intra-class correlation coefficients for reliability research. J Chiropr Med 15:155–163

Kress BC, Cummings WJ (2017a) 11-1: Invited paper: towards the ultimate mixed reality experience—HoloLens display architecture choices. SID Symp Dig Tech Pap 48:127–131

Kress BC, Cummings WJ (2017b) Optical architecture of HoloLens mixed reality headset. Digit Opt Technol 2017:103350K

Lalla R, Brown TL, Griffiths RW (2003) Where to draw the line: the error in marking surgical excision margins defined. Br J Plast Surg 56:603–606

Lopes-Ferreira D, Neves H, Queiros A, Faria-Ribeiro M, Peixoto-de-Matos SC, González-Méijome JM (2013) Ocular dominance and visual function testing. Biomed Res Int 2013:238943

Luparia A, Mariscotti G, Durando M, Ciatto S, Bosco D, Campanino PP, Castellano I, Sapino A, Gandini G (2013) Accuracy of tumour size assessment in the preoperative staging of breast cancer: comparison of digital mammography, tomosynthesis, ultrasound and MRI. Radiol Med 118:1119–1136

Luzon JA, Stimec BV, Bakka AO, Edwin B, Ignjatovic D (2020) Value of the surgeon's sightline on hologram registration and targeting in mixed reality. Int J Comput Assist Radiol Surg 15:2027–2039

Mattos LS, Caldwell DG, Peretti G, Mora F, Guastini L, Cingolani R (2016) Microsurgery robots: addressing the needs of high-precision surgical interventions. Swiss Med Wkly 146:w14375

Park S, Bokijonov S, Choi Y (2021) Review of microsoft HoloLens applications over the past five years. Appl Sci 11:7259

Pérez-Pachón L, Poyade M, Lowe T, Gröning F (2020) Image overlay surgery based on augmented reality: a systematic review. In: Rea PM (ed) Biomedical visualisation. Springer

Pérez-Pachón L, Sharma P, Brech H, Gregory J, Lowe T, Poyade M, Gröning F (2021) Effect of marker position and size on the registration accuracy of HoloLens in a non-clinical setting with implications for high-precision surgical tasks. Int J Comp Assist Radiol Surg 16:955–966

Poortmans PM, Collette L, Horiot JC, Van den Bogaert WF, Fourquet A, Kuten A, Noordijk EM, Hoogenraad W, Mirimanoff RO,

Pierart M, Van Limbergen E, Bartelink H (2009) Impact of the boost dose of 10 Gy versus 26 Gy in patients with early stage breast cancer after a microscopically incomplete lumpectomy: 10-year results of the randomised EORTC boost trial. Radiother Oncol 90:80–85

Pratt P, Ives M, Lawton G, Simmons J, Radev N, Spyropoulou L, Amiras D (2018) Through the HoloLens™ looking glass: augmented reality for extremity reconstruction surgery using 3D vascular models with perforating vessels. Eur Radiol Exp 2:2

Reiss MR (1997) Ocular dominance: some family data. Laterality 2:7–16

Richmond JD, Davie RM (1987) The significance of incomplete excision in patients with basal cell carcinoma. Br J Plast Surg 40:63–67

Ríos-Buceta L (2007) Management of basal cell carcinomas with positive margins. In: Actas dermosifiliogr, pp 679–687

Sadideen H, Alvand A, Saadeddin M, Kneebone R (2013) Surgical experts: Born or made? Int J Surg 11:773–778

Shao P, Ding H, Wang J, Liu P, Ling Q, Chen J, Junbin Xu, Zhang S, Ronald Xu (2014) Designing a wearable navigation system for image-guided cancer resection surgery. Ann Biomed Eng 42:2228–2237

Sheoran A, Garg A, Yadav U, Kundu ZS, Sherawat R, Singla M, Nemani M, Wason D, Kulaar HS, Singha SB (2022) Outcomes of wide resection of soft-tissue sarcoma of the extremity: a retrospective analysis. Cureus 14:e27329

Sondak VK, Zager JS (2010) Who is to blame for false-negative sentinel node biopsies in melanoma? Ann Surg Oncol 17:670–673

Sugiura H, Tsukushi S, Yoshida M, Nishida Y (2018) What is the success of repeat surgical treatment of a local recurrence after initial wide resection of soft tissue sarcomas? Clin Orthop Relat Res 476:1791–1800

Telfer NR, Colver GB, Morton CA (2008) Guidelines for the management of basal cell carcinoma. Br J Dermatol 159:35–48

Waljee JF, Hu ES, Newman LA, Alderman AK (2008) Predictors of re-excision among women undergoing breast-conserving surgery for cancer. Ann Surg Oncol 15:1297

Wilson JL, Morritt AN, Morrison WA (2009) Chapter 12—avoiding complications. In: Wei F-C, Mardini S (eds) Flaps and reconstructive surgery. W.B. Saunders, Edinburgh

Zhang J, Lu V, Khanduja V (2023) The impact of extended reality on surgery: a scoping review. Int Orthop 47:611–621